sample. By way of estimate, we note that $\hbar/\tau_s \sim 10^{-6}$ K; the experimental data on $\hbar/\tau_{vv}$ in the range from 10^{-1} to 10^{-4} K are as yet of low reliability. This question is purely academic, however, because such low temperatures are many orders of magnitude below the currently accessible level.

In summary, theory suggests an extraordinary picture, where the metal–insulator transition occurs at a finite temperature and is a true quantum transition, but, strictly speaking, the metallic state that results does not survive the $T = 0$ limit (provided the 2D system does not make a spontaneous transition to another universality class — due to the formation of local magnetic moments [48] or of a two-phase microemulsion state [49], for example). Other remaining questions are whether the phase diagram of a 2D metal–insulator transition will be valid, at least in general terms, for realistic cases such as $n_v = 6$, 2 or 1, and down to what temperatures a 2D metal can exist in real-life systems.

Acknowledgements The above experimental study by the present author and coworkers was supported by grants from the RFBR, INTAS, RAS Presidium programs, RAS Physics Sciences Division programs, and the President's program for leading scientific schools.

References

1. Al'tshuler B L, Aronov A G, in *Electron-Electron Interactions in Disordered Systems* (Modern Problems in Condensed Matter Sciences, Vol. 10, Eds A L Efros, M Pollak) (Amsterdam: North-Holland, 1985) p. 1
2. Lee P A, Ramakrishnan T V *Rev. Mod. Phys.* **57** 287 (1985)
3. Altshuler B L, Aronov A G, Khmelnitskii D E, Larkin A I, in *Kvantovaya Teoriya Tverdogo Tela* (Quantum Theory of Solids) (Ed. I M Lifshits) (Moscow: Mir, 1982) [Translated into English (Moscow: Mir Publ., 1982) p. 130]
4. Abrahams E et al. *Phys. Rev. Lett.* **42** 673 (1979)
5. Wigner E *Phys. Rev.* **46** 1002 (1934)
6. Tanatar B, Ceperley D M *Phys. Rev. B* **39** 5005 (1989)
7. Chui S T (Ed.) *Physics of 2D Quantum Electron Solids* (Cambridge, MA: International Press, 1994)
8. D'Iorio M, Pudalov V M, Semenchinsky S G *Phys. Lett. A* **150** 422 (1990)
9. D'Iorio M, Pudalov V M, Semenchinsky S G *Phys. Rev. B* **46** 15992 (1992)
10. Pudalov V M, D'Iorio M, Campbell J W *Pis'ma Zh. Eksp. Teor. Fiz.* **57** 592 (1993) [*JETP Lett.* **57** 608 (1993)]
11. Kravchenko S V et al. *Phys. Rev. Lett.* **75** 910 (1995)
12. Khmelnitskii D E *Phys. Lett. A* **106** 182 (1984)
13. Laughlin R B *Phys. Rev. Lett.* **52** 2304 (1984)
14. Kravchenko S V et al. *Phys. Rev. B* **50** 8039 (1994)
15. Kravchenko S V et al. *Phys. Rev. B* **51** 7038 (1995)
16. Pudalov V M et al. *Pis'ma Zh. Eksp. Teor. Fiz.* **68** 415 (1998) [*JETP Lett.* **68** 442 (1998)]; *Physica E* **3** 79 (1998)
17. Pudalov V M, in *The Electron Liquid Paradigm in Condensed Matter Physics* (Proc. of the Intern. School of Physics Enrico Fermi, Course CLVII, Eds G F Giuliani, G Vignale) (Amsterdam: IOS Press, 2004) p. 335; cond-mat/0405315
18. Abrahams E, Kravchenko S V, Sarachik M P *Rev. Mod. Phys.* **73** 251 (2001)
19. Altshuler B L, Maslov D L, Pudalov V M *Physica E* **9** 209 (2001)
20. Pudalov V M, Gershenson M, Kojima H, in *Fundamental Problems of Mesoscopic Physics*: *Interactions and Decoherence* (NATO Sci. Ser., Ser. II, Vol. 154, Eds I V Lerner, B L Altshuler, Y Gefen) (Dordrecht: Kluwer Acad. Publ., 2004) Ch. 19, p. 309
21. Shashkin A A *Usp. Fiz. Nauk* **175** 139 (2005) [*Phys. Usp.* **48** 129 (2005)]
22. Okamoto T et al. *Phys. Rev. Lett.* **82** 3875 (1999)
23. Pudalov V M et al. *Phys. Rev. Lett.* **88** 196404 (2002)
24. Zhu J et al. *Phys. Rev. Lett.* **90** 056805 (2003)
25. Proskuryakov Y Y et al. *Phys. Rev. Lett.* **89** 076406 (2002)
26. Shashkin A A et al. *Phys. Rev. B* **66** 073303 (2002)
27. Vitkalov S A et al. *Phys. Rev. B* **67** 113310 (2003)
28. Pudalov V M et al. *Phys. Rev. Lett.* **91** 126403 (2003); *Phys. Rev. Lett.* **93** 269704 (2004)
29. Vitkalov S A et al. *Phys. Rev. Lett.* **87** 086401 (2001)
30. Shashkin A A et al. *Phys. Rev. Lett.* **87** 086801 (2001)
31. Vitkalov S A, Sarachik M P, Klapwijk T M *Phys. Rev. B* **65** 201106 (2002)
32. Yoon J et al. *Phys. Rev. Lett.* **84** 4421 (2000)
33. Tutuc E et al. *Phys. Rev. Lett.* **86** 2858 (2001)
34. Tutuc E et al. *Phys. Rev. B* **67** 241309(R) (2003)
35. Tutuc E, Melinte S, Shayegan M *Phys. Rev. Lett.* **88** 036805 (2002)
36. Pudalov V M et al. *Phys. Rev. Lett.* **88** 076401 (2002)
37. Prus O et al. *Phys. Rev. B* **67** 205407 (2003)
38. Zala G, Narozhny B N, Aleiner I L *Phys. Rev. B* **64** 214204; **65** 020201 (2001)
39. Gornyi I V, Mirlin A D *Phys. Rev. B* **69** 045313 (2004)
40. Olshanetsky E B et al. *Phys. Rev. B* **68** 085304 (2003)
41. Punnoose A, Finkel'stein A M *Phys. Rev. Lett.* **88** 16802 (2002)
42. Iordanski S V, Kashuba A *Pis'ma Zh. Eksp. Teor. Fiz.* **76** 660 (2002) [*JETP Lett.* **76** 563 (2002)]
43. Pudalov V M et al. *Phys. Rev. B* (to be published)
44. Finkel'shtein A M *Zh. Eksp. Teor. Fiz.* **84** 168 (1983); **86** 367 (1984) [*Sov. Phys. JETP* **57** 97 (1983); **59** 212 (1984)]; Finkel'stein A M *Z. Phys. B* **56** 189 (1984); *Sov. Sci. Rev. Sect. A Phys. Rev.* (Ed. I M Khalatnikov) **14** (2) 3 (1990)
45. Castellani C et al. *Phys. Rev. B* **30** 527 (1984)
46. Castellani C et al. *Phys. Rev. B* **30** 1596 (1984)
47. Punnoose A, Finkel'stein A M *Science* **310** 289 (2005)
48. Dobrosavljević V et al. *Phys. Rev. Lett.* **79** 455 (1997)
49. Spivak B, Kivelson S A *Phys. Rev. B* **70** 155114 (2004)

PACS numbers: 71.10.Ca, **71.27 + a**, 73.43.Cd
DOI: 10.1070/PU2006v049n02ABEH005922

Two-dimensional multicomponent electron gas as a model for silicon heterostructures

S V Iordanskii, A Kashuba

1. Introduction

Two-dimensional electron gas in a Si-heterostructure can vary very widely in density [1]. Effects due to the electron–electron Coulomb interaction are determined by the dimensionless ratio of the average Coulomb energy to the electron kinetic energy, $r_s = e^2 m/\sqrt{\pi n}\,\hbar^2$, with n being the electron density. For relatively large r_s, $1 < r_s < 10$, Si-MOSFETs (metal-oxide-semiconductor field-effect transistors) undergo a transition from the metallic (growing) to dielectric (falling) conductivity with decreasing temperature [2] and demonstrate an increase in the effective mass and magnetic susceptibility with increasing r_s [3, 4]. Because of the lack of exactly solvable models for large r_s, various phenomenological models have come to the fore. The electron–hole plasma observed in a three-dimensional (3D) electron–hole droplet in Si and Ge is also characterized by comparatively large values of r_s. As shown in the pioneering work of Ref. [5], the multivalley band structure leads to the existence in these semiconductors of a 'metallized' electron–hole plasma in the region of relatively large r_s (see also Ref. [6]). One would expect that allowing for many valleys in two-dimensional (2D) Si-heterostructures would lead to better agreement with experiment compared with Landau's Fermi-liquid theory with its small-r_s corrections to the theory of a dense electron gas. The Fermi-liquid theory predictions for Si-heterostructures are in quantitative disagreement with experiment even

at moderate values of r_s. For example, the theory of a dense electron gas predicts an increase in the effective mass at small r_s, [7],

$$\frac{m^*}{m} = 1 - \frac{r_s}{\pi} \log\left(\frac{1}{r_s}\right), \tag{1}$$

whereas Shubnikov – de Haas measurements [8, 9] yield

$$\frac{m^*}{m} \approx 1 + 0.08 r_s \,. \tag{2}$$

Another point to note concerns charged excitations on the lowest filled Landau level. Experimentally, their activation energy (which is small according to the magnetoconductance measurements in Ref. [10]) is roughly proportional to the magnetic field H, whereas theoretically [11], it must be proportional to its square root, $e^2\sqrt{eH/\hbar c}$ (the same as the electron – electron interaction). These phenomena are observed at $1.5 < r_s < 3$, which is far from the metal – insulator transition. We show that a systematic model of a 2D multicomponent high-density electron gas gives qualitative agreement with the experimental data for highest-purity silicon heterostructures.

Electron states in silicon have valley degeneracy [1] that corresponds to different band energy maxima. For the (1,0,0)-oriented heterostructure plane in a silicon crystal, there are $N = 4$ equivalent, orthogonal spin-valley electron states that differ by a factor $\exp(\pm \mathrm{i} Q z)$ in the perpendicular direction with atomic wave vector Q. For the $(1, 1, 1)$ orientation, the spin-valley degeneracy is $N = 12$. A 3D electron gas in the limit $N \to \infty$ was first treated in Ref. [12].

2. Multicomponent Fermi liquid

A systematic theory can be developed in the limit $1 > r_s \gg N^{-3/2}$, where it differs quite substantially from the $r_s \ll N^{-3/2}$ limit theory, which yields standard Fermi-liquid results. The model is described by the Hamiltonian

$$\hat{H} = \frac{1}{2m} \int \psi_\alpha^\dagger(\mathbf{r}) \left(-\mathrm{i}\hbar\nabla + \frac{e}{c}\,\mathbf{A}(\mathbf{r}) \right)^2 \psi_\alpha(\mathbf{r})\, \mathrm{d}^2\mathbf{r} + \frac{1}{2} \iint \frac{e^2}{|\mathbf{x} - \mathbf{r}|}\, \psi_\alpha^\dagger(\mathbf{x})\, \psi_\beta^\dagger(\mathbf{r})\, \psi_\beta(\mathbf{r})\, \psi_\alpha(\mathbf{x})\, \mathrm{d}^2\mathbf{x}\, \mathrm{d}^2\mathbf{r} \,, \tag{3}$$

where valley-to-valley transitions are not allowed, α and β are conserved ($\alpha, \beta \leqslant N$) as in the exchange approximation, and the mass m is isotropic. It is assumed that there is a compensating positive charge at a large distance from the heterostructure plane. The summation is over the spin-valley indices.

The effect of a multivalley structure primarily shows up as a highly screened Coulomb interaction. The Coulomb interaction gives rise to polarization effects in each valley, thus decreasing interaction between electrons residing in the same valley. Accordingly, even though $r_s^{(1)}$ calculated only for the electrons in one valley may be large, $r_s(N)$ for all the N valleys is small, enabling expressions for physical properties to be systematically expanded in powers of $r_s(N)$. For our purposes, the Matsubara diagram technique as applied in its low-temperature limit [13] is sufficient. In the 2D limit (i.e., at distances much longer than the heterostructure thickness), the Coulomb interaction between electrons in the heterostructure has the Fourier component

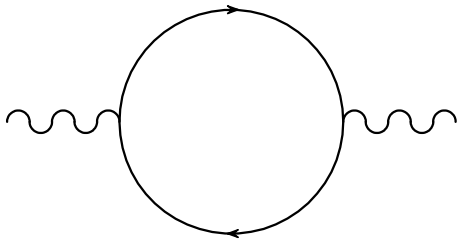

Figure 1. Polarization bubble. Electron propagators and the Coulomb interaction are represented by arrowed and wavy lines, respectively.

$$V(\mathbf{q}) = \frac{2\pi e^2}{|\mathbf{q}|} \,. \tag{4}$$

Calculating the effective interaction requires knowing the electron polarization by the interaction field in all the valleys, which can be depicted by the diagram in Fig. 1, showing the creation of electron – hole pairs by the Coulomb interaction. In this figure, the normal line represents the free electron Green's function

$$G_\alpha^0(\varepsilon, \mathbf{p}) = \frac{1}{\mathrm{i}\varepsilon - (\varepsilon_\alpha(\mathbf{p}) - \mu)} \,, \tag{5}$$

where $\varepsilon(\mathbf{p}) = p^2/2m$ is spin- and valley-independent, and the wavy line is for the Fourier component of Coulomb interaction (4). The calculation of the effective interaction involves summation over all valleys and requires that the polarization effects of all orders be included. This means using the random-phase approximation (RPA) and summing all diagrams with the number of polarization bubbles being maximum for a given number of interaction lines:

$$V_{\mathrm{eff}}(\omega, q) = \frac{2\pi e^2/q}{1 + (2\pi e^2/q)\, \Pi(\omega, q)} \,, \tag{6}$$

where $\Pi(\omega, q)$ corresponds to the diagrams for a single polarization bubble. Because the one-valley electron density n_1 is small compared with the total density $n = N n_1$, the Fermi momentum p_F is also small compared with the momentum transfer q. In the limit $q \gg p_F$, the quantity $\Pi(\omega, q)$ is easily calculated to be

$$\Pi(\omega, q) = \frac{2n\varepsilon(q)}{\omega^2 + \varepsilon^2(q)} \,, \tag{7}$$

and the effective Coulomb interaction becomes

$$D(\omega, q) = \frac{2\pi e^2}{q}\, \frac{\omega^2 + \varepsilon^2(q)}{\omega^2 + \varepsilon^2(q) + 4\pi e^2 n \varepsilon(q)/q} \,. \tag{8}$$

The poles of $D(\omega, q)$ correspond to zeros of the dielectric constant and yield the plasmon excitation energy

$$\omega(q) = \frac{\hbar^2}{2m} \sqrt{q^2 + q_0^3 q} \,, \tag{9}$$

where $q_0^3 = 8\pi e^2 n m/\hbar^2$ is the characteristic momentum of the effective interaction. Thus, the plasmon energy turns out to be large compared to the kinetic energy ε_F, making the effective interaction small.

Diagram calculations can be interpreted in terms of a picture in which plasmons, described by the propagator $D(\omega, q)$, interact with one another via closed loops containing more than two electron lines. A vertex containing $k > 2$ plasmon lines with large momenta $\sim q_0$ and with frequencies $\omega_0 \sim q_0^2/2m$ is of the order of $V_k \sim n/\omega_0^{k-1}$. With these estimates, it is possible to classify all the diagrams by powers of $r_s^{2/3}$. The correlation energy per unit volume calculated in the next-to-leading order is given by

$$E_c = -\left(2.03191\ r_s^{4/3} - 0.156(1)\ r_s^2\right)\ \frac{n^2}{m}\,. \tag{10}$$

But it is more interesting to calculate corrections to the electron Green's function

$$G^{-1}(\varepsilon, \mathbf{p}) = \mathrm{i}\varepsilon - \left(\varepsilon(\mathbf{p}) - \mu\right) - \Sigma(\varepsilon, \mathbf{p})\,. \tag{11}$$

Because of the small magnitude of the screened interaction, the mass operator may be calculated in the first order in the plasmon operator $D(\omega, q)$,

$$\Sigma(\varepsilon, \mathbf{p}) = -\int D(\omega, \mathbf{q})\, G(\varepsilon + \omega, \mathbf{p} + \mathbf{q})\ \frac{\mathrm{d}\omega\, \mathrm{d}^2\mathbf{q}}{(2\pi)^3}\,. \tag{12}$$

Because of the large values of the plasmon momentum and energy, the integral can be evaluated by taking $\varepsilon \ll \omega$ and $p \ll q$, and the Green's function near the Fermi surface takes the form

$$G(\varepsilon, p) = \frac{Z(p_F)}{\mathrm{i}\varepsilon - \varepsilon_R(p) + \mu}\,, \quad \varepsilon_R(p) = \frac{p_F}{m^*}\,(p - p_F)\,, \tag{13}$$

where, for small r_s,

$$\frac{m}{m^*} = 1 - \frac{1}{10\sqrt{\pi}}\ \Gamma\left(\frac{1}{3}\right)\Gamma\left(\frac{7}{6}\right)\ r_s^{2/3} + O(r_s^{4/3})\,,$$

$$Z^{-1}(p_F) = 1 + \frac{1}{2\sqrt{\pi}}\ \Gamma\left(\frac{1}{3}\right)\ \Gamma\left(\frac{7}{6}\right)\ r_s^{2/3} + O(r_s^{4/3})\,, \tag{14}$$

where $\Gamma(v)$ is the gamma function.

Similarly, for the spin magnetic susceptibility, we obtain

$$\frac{\chi^*}{\chi} = \frac{m^*}{m}\,, \tag{15}$$

where $\chi = m/2\pi\hbar^2$ is the susceptibility of a 2D Fermi gas of Pauli. Figure 2 compares experimental data on m^*/m and χ^*/χ [14] with theoretical predictions. It can be seen that the effective mass shows good agreement, whereas the susceptibility is somewhat underpredicted — due to exchange effects, which are absent in the theory at $N = \infty$ but should show up in real silicon at $N = 4$. (We also note that at $r_s \approx 9$, a Si-MOSFET undergoes a metal–insulator transition, which is beyond our theoretical model).

We note that the effective mass and magnetic susceptibility renormalization in Landau's Fermi liquid theory are related to the properties of the (scattering-angle-dependent) effective interaction function of the particles involved [15]. Unlike this, in a multicomponent gas, these Fermi-liquid parameters are determined by the properties of plasmons, whose energies and momenta are much larger than those of the Fermi-surface electrons. Besides, the small Fermi momentum together with strong screening effects prevents Friedel density oscillations from occurring in a multicomponent gas.

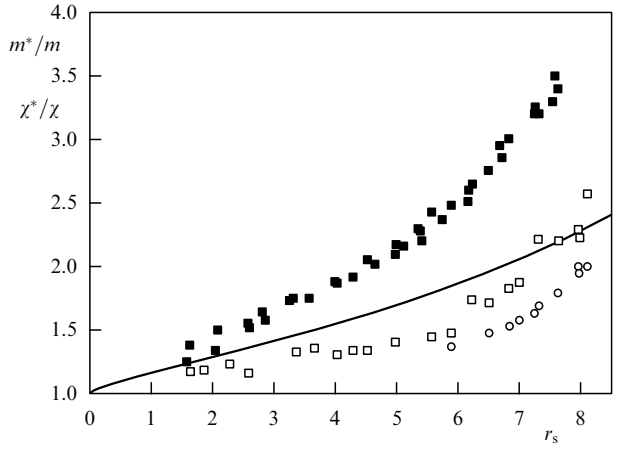

Figure 2. Experimental data for the magnetic susceptibility χ^*/χ (black squares) and effective mass m^*/m (white circles and squares). Solid curve: the susceptibility and mass obtained from the multicomponent model.

To show this, we note that the induced charged density in a multicomponent gas is given by

$$\delta n(\mathbf{r}) = \int \frac{2\pi e^2 \Pi(0, q)}{q + 2\pi e^2 \Pi(0, q)}\ \exp(\mathrm{i}\mathbf{q}\mathbf{r})\ \frac{\mathrm{d}^2\mathbf{q}}{(2\pi)^2}$$

$$= \int_0^\infty \frac{q_0^3}{q^3 + q_0^3}\ J_0(qr)\ \frac{q\,\mathrm{d}q}{2\pi}\,. \tag{16}$$

The function $\delta n(\mathbf{r})$ is concentrated at $r \sim 1/q_0 \ll 1/p_F$, where it has one zero, and decreases exponentially with distance. The outer charge is fully screened,

$$\int \delta n(\mathbf{r})\, \mathrm{d}^2\mathbf{r} = 1\,. \tag{17}$$

Friedel oscillations [15] are related to the singularity at $q = 2p_F$ [which is neglected in Eqn (7)] and have the period $\pi\hbar/p_F$ and the amplitude $\sim p_F^2/N$, which is vanishingly small in the limit $N \to \infty$. We therefore conclude that many Fermi surface features are absent in a multicomponent gas.

3. Adding a magnetic field

The multicomponent model can be extended to include a large external magnetic field perpendicular to the heterostructure plane. Then the ground state of the system is one with the lowest Landau level filled. We suppose that of N spin-valleys present, only $1 \ll v < N$ have their zeroth level completely filled. Although the system does not make real transitions to higher Landau levels, the virtual transitions it does make screen the Coulomb interaction as before. The unperturbed electron Green's function for one valley can be written as the sum

$$G_0(\varepsilon, \mathbf{r}, \mathbf{r}') = \sum_{s,p} \frac{1}{\mathrm{i}\varepsilon - (s + 1/2)\,\omega_H + \mu}\ \Phi_{sp}(\mathbf{r})\, \Phi_{sp}^*(\mathbf{r}')\,, \tag{18}$$

where s is the Landau index, Φ_{sp} is the Landau-level wave function, and ω_H is the cyclotron frequency. The polarization operator is calculated to be

$$\Pi(\omega, \mathbf{q}) = \frac{v}{2\pi} \sum_{s=1}^{\infty} \frac{q^{2s}}{2^s\ s!}\ \frac{2s\omega_H}{\omega^2 + \omega_H^2 s^2}\ \exp\left(-\frac{q^2}{2}\right), \tag{19}$$

(in a system of units where the magnetic length $l_H = 1$ and $e = c$, $\omega_H = 1/m$). Such a special form of the polarization operator is because the electron – hole polarization loop in the coordinate representation is a function of $(\mathbf{r} - \mathbf{r}')$ if an external magnetic field is present.

A plasmon propagator, like $D(\omega, q)$, has the form (6). In the presence of a completely filled Landau level in $\Pi(\omega, q)$ valleys, additional energy comes into play due to the electron being transferred from an occupied valley to the same level in an empty valley, with a hole left behind. This energy has its origin in exchange effects and corresponds to a spin wave in the one-valley case. This is a neutral excitation, and one which is characterized by a momentum, despite the presence of a magnetic field. In this situation, an exchange exciton forms. At a large momentum, the electron and the hole are far apart, their interaction is negligible, and they can therefore be considered free — leading to the conclusion that their energy is the activation energy for charge excitations, the electron energy difference between the empty and occupied valleys. This energy can be calculated to give

$$\Delta = \int D(0,q)\ \exp\left(-\frac{q^2}{2}\right)\frac{\mathrm{d}^2\mathbf{q}}{(2\pi)^2} = \frac{\hbar\omega_H}{\nu}\left(\log(r_s\nu^{3/2}) + 0.277\right), \qquad (20)$$

($r_s = \sqrt{2}e^2/\omega_H l_H\sqrt{\nu}$), showing that the activation energy is approximately proportional to the magnetic field and is small in the limit of large ν. The linear behavior agrees qualitatively with the magneto-conductance measurements of the activation energy [10], but Eqn (20) greatly overestimates the activation energy — possibly because the extrapolation to relatively large r_s is itself a rather crude procedure or because factors such as a finite thickness of the 2D layer or the image force from the metal gate were not taken into account.

The energy of an exchange exciton at low momentum Q is calculated in a similar way, giving

$$\omega(Q) = J(Ql_H)^2, \quad J = 0.6613\ \frac{\omega_H}{\nu}\,. \qquad (21)$$

Thus, we see that the exchange constant J is also screening-suppressed and varies linearly with the magnetic field.

Some of the results in this paper were previously presented in Ref. [16].

Acknowledgements. This work was supported by RFBR grants 03-02-17229a and 0501-16553a.

References

1. Ando T, Fowler A B, Stern F *Rev. Mod. Phys.* **54** 437 (1982)
2. Abrahams E, Kravchenko S V, Sarachik M P *Rev. Mod. Phys.* **73** 251 (2001)
3. Pudalov V M et al. *Phys. Rev. Lett.* **88** 196404 (2002)
4. Shashkin A A et al. *Phys. Rev. B* **66** 073303 (2002)
5. Bagaev V S et al. *Pis'ma Zh. Eksp. Teor. Fiz.* **10** 309 (1969) [*JETP Lett.* **10** 195 (1969)]
6. Jeffries C D, Keldysh L V (Eds) *Electron-Hole Droplets in Semiconductors* (Modern Problems in Condensed Matter Sciences, Vol. 6) (Amsterdam: North-Holland Publ. Co., 1983)
7. Gell-Mann M, Brueckner K A *Phys. Rev.* **106** 364 (1957); Sawada K *Phys. Rev.* **106** 372 (1957); Gell-Mann M *Phys. Rev.* **106** 369 (1957)
8. Smith J L, Stiles P J *Phys. Rev. Lett.* **29** 102 (1972)
9. Okamoto T et al. *Phys. Rev. Lett.* **82** 3875 (1999)
10. Khrapai V S, Shashkin A A, Dolgopolov V T *Phys. Rev. B* **67** 113305 (2003)
11. Bychkov Yu A, Iordanskii S V, Eliashberg G M *Pis'ma Zh. Eksp. Teor. Fiz.* **33** 152 (1981) [*JETP Lett.* **33** 143 (1981)]; Kallin C, Halperin B I *Phys. Rev. B* **30** 5655 (1984)
12. Takada Y *Phys. Rev. B* **43** 5962 (1991)
13. Abrikosov A A, Gor'kov L P, Dzyaloshinskii I E *Metody Kvantovoi Teorii Polya v Statisticheskoi Fizike* (Methods of Quantum Field Theory in Statistical Physics) (Moscow: Dobrosvet, 1998) [Translated into English (New York: Dover Publ., 1975)]
14. Pudalov V M, Gershenson M E, Kojima H, in *Fundamental Problems of Mesoscopic Physics*: *Interactions and Decoherence* (NATO Sci. Ser., Ser. II, Vol. 154, Eds I V Lerner, B L Altshuler, Y Gefen) (Dordrecht: Kluwer Acad. Publ., 2004)
15. Pines D, Nozières P *The Theory of Quantum Liquids* (New York: W.A. Benjamin, 1966)
16. Iordanski S V, Kashuba A *Pis'ma Zh. Eksp. Teor. Fiz.* **76** 660 (2002) [*JETP Lett.* **76** 563 (2002)]

PACS numbers: **71.27.+a**, **71.30.+h**, 72.15.Rn

DOI: 10.1070/PU2006v049n02ABEH005923

Interaction effects in the transport and magnetotransport of two-dimensional electrons in AlGaAs/GaAs and Si/SiGe heterojunctions

E B Olshanetskii, V Renard, Z D Kvon, I V Gornyi, A I Toropov, J C Portal

1. Introduction

Localization- and interaction-induced quantum corrections to the conductivity of two-dimensional (2D) electron systems [1, 2] have been the subject of considerable study since as long as a quarter century ago. It should be noted that weak localization effects do not present any problems, and that their associated anomalous magnetoresistance very soon became a powerful tool for probing the low-temperature properties of disordered metallic systems, from thin superconducting films to near-surface 2D layers in semiconductors. Unlike this, the behavior of interaction effects remained the subject of continuous heated debate — primarily in connection with how they influence the metal – insulator transition in a 2D electron system [3]. What made things especially topical was the discovery [4] that a high-mobility 2D electron gas in silicon MOS (metal-oxide-semiconductor) transistors exhibits states whose conductivity increases anomalously with lowering the temperature, which is entirely inconsistent with theoretical expectations [1, 2]. This situation has stimulated new ideas in the theory of interaction-induced quantum corrections and has recently led to its further development in Refs [5 – 7], which identified two regimes — the diffusion one (for $T\tau/\hbar \ll 1$) and the ballistic one (for $T\tau/\hbar \gg 1$) — in the behavior of quantum corrections. Both regimes are of the same nature, i.e., are determined by single and multiple scattering from impurities and from the Friedel oscillations in their screening charge. Both mechanisms had already been know before Refs [5 – 7]. The first mechanism [1, 2] was thought to be related to the quantum corrections due to the interference of interacting electrons (see above), and the second was linked to the temperature dependence of screening due to the singularity in 2D screening near $q \approx 2k_F$ [8] and was considered to be a temperature-dependent part of the one-electron transport time, unrelated to quantum interference.